

Received 8 October 2023, accepted 1 November 2023, date of publication 13 November 2023,
date of current version 20 November 2023.

Digital Object Identifier 10.1109/ACCESS.2023.3332478

RESEARCH ARTICLE

Soccer Robot Localization Detection Model Based on Monte Carlo Particle Filter and Template Matching Algorithm

LI XIAO 

Department of Basic Teaching, Henan Logistics Vocational College, Zhengzhou, Henan 453000, China
e-mail: 13838346626@163.com


ABSTRACT With the continuous development of information technology, artificial intelligence and location detection technology have gradually penetrated various systems. The research progress in the field of humanoid robots is on paper, but there are still some defects that limit the performance of robots in some application scenarios. In order to solve the problem of feature recognition and robot self-localization in football field, this paper proposes a soccer robot localization detection model based on Monte Carlo particle filter and template matching algorithm. The model uses particle filter for robot positioning to achieve the purpose of global visual positioning and navigation, in order to meet the needs of real-time and accuracy during the competition. The image is preprocessed by template matching, and the feature information and edge information are extracted to recognize the target. The results show that the highest accuracy of the proposed algorithm is 0.895, and its accuracy is 0.99. When the recall rate reaches 1, the accuracy rate can still be maintained at 0.43, which verifies the effectiveness and practicability of the localization detection model under the use of this algorithm.

INDEX TERMS Monte Carlo particle filter, location detection, template matching algorithm, humanoid robots, site feature recognition.

I. INTRODUCTION

Intelligent robots play an important role in serving the major needs of the country, leading the development of the national economy and ensuring national defense security [1]. With the industrial development in the new era, the world has gradually become a strategic goal with intelligent manufacturing as the main body. As an important carrier of intelligent manufacturing, intelligent robots have promoted the development of high-end, intelligent and information technology in the in-depth implementation of the deployment of manufacturing power war [2]. Mobile robot technology is a multifunctional integrated system involving robotics, image processing, artificial intelligence, automatic control and information communication [3]. Robot vision technology is the foundation of this field. Images are acquired through the

robot's visual sensing, and the images are digitally processed to control the robot's actions [4]. Therefore, vision-based robot technology is widely used in robot navigation, road stiffness planning, target tracking and motion control [5]. Therefore, aiming at image preprocessing and feature extraction, this study proposed a soccer robot positioning detection model based on Monte Carlo Particle Filter (MCPF) and Template Matching (TM). In order to improve the accuracy of global self-positioning of soccer robots. The research content is mainly divided into five parts. The first part is the introduction, which describes the involvement of artificial intelligence in People's Daily life under the background of the rapid development of science and technology. The second part is the literature review, the realization of MCPF, TM and robot positioning detection model in various fields, and the research status of many scholars on this technology. In the third part, MCPF and TM algorithms are described, and the global self-positioning detection of the robot is

The associate editor coordinating the review of this manuscript and approving it for publication was Abdel-Hamid Soliman .

analyzed. The first section analyzes the MCPF positioning algorithm and summarizes its principle; the second section is the application of TM algorithm in image processing and feature recognition; the third section is the construction of the self-positioning detection model of soccer robot based on MCPF and TM algorithms. In the fourth part, the performance of the robot positioning detection model is tested, and the evaluation indexes of accuracy and recall rate in the positioning detection model are statistically analyzed. The fifth part is the summary and prospect of the research methods and results. The MCPF algorithm estimates the state of the system based on a probability distribution to generate a series of particles for prediction and update to find the particles that are closest to the actual system state. Template matching, as an algorithm based on image recognition, can match the template that is most similar to the current image in a set of preset templates, so as to realize the location of the object. The MCPF is used to generate a large number of particles that represent the possible location of the robot. Then, through the acquired real-time image data, the template matching algorithm is used to match the preset robot template to find the possible robot position. Using the matching results, the MCPF particles are reweighted to remove the particles that are far from the template matching results, leaving those particles that are consistent with the actual observation, in order to obtain a more accurate robot position prediction. The combination of MCPF and template matching algorithm is that MCPF provides multiple prediction locations based on possibility, while template matching algorithm provides an effective filtering mechanism according to the actual situation, selectively retaining those predictions that are more consistent with the actual situation, so as to achieve a better positioning effect.

II. RELATED WORKS

Positioning humanoid robots is very important. Among various key technologies in SR, many scholars have achieved considerable research results in global positioning of robots in competitions. Jiao Z et al. proposed a clustering similarity particle filter (PF) based on state trajectory consistency. This can be used to measure the state trajectories of sampled particles and actual systems. The importance weights of the first-order Markov model were updated using the measurement results. The improved PF is superior to the traditional filter in estimation accuracy, efficiency and robustness, effectively reducing the adverse effects of particle degradation [6]. Liu Q et al. proposed a map based positioning system for self-positioning of autonomous vehicle in urban environments. The system consists of a location map mapping method and a three-dimensional curvature feature point Monte Carlo positioning algorithm. This algorithm can use the 3 Dimensions (3D) point cloud map generated by our mapping method to provide accurate positioning for autonomous vehicle [7]. Jasra A and Ballesio M estimate the static parameters of a continuous time state space model to obtain unbiased estimates of the logarithmic likelihood

gradient. The application of double random scheme and coupling condition PF in the second level randomization helps to promote the application of gradient based estimation algorithm [8]. Hu B et al. proposed an improved PF algorithm, and estimated the importance probability function of the generated PF through the improved iterative Kalman filter. The algorithm can use fewer sampled particles to approach the posterior probability distribution of state more closely, which improves the real-time performance. The positioning algorithm accuracy meets the requirements of real-time positioning of restaurant service robots [9].

In the complex competition environment of SR, it is crucial to preprocess images and extract the necessary feature information for target recognition. TM can recognize the edge information of features very clearly, and many scholars have also studied this topic. Liang S and Li Y studied the tracking feature matching of basketball players' detection, recognition, and prediction in game videos, which mainly includes four parts. They include motion object detection, recognition, basketball trajectory feature matching, and player trajectory feature matching. Kalman filter is used to study the characteristics of matching basketball trajectory, predict the Basketball positions at the time of occlusion, and realize the matching of occlusion trajectory. This algorithm fully utilizes the player's color information and achieves real-time performance [10]. Niu Y et al. proposed the optimized Genetic Algorithm (GA) TM and compared the effect of traditional GA applied to Computed Tomography (CT) images of patients with COVID-19. This algorithm can improve the accuracy of pneumonia detection and reduce the false positive rate. Compared with the general group, the total T lymphocyte count of patients in the severe group decreased sharply. The anxiety and depression scores of internal medicine patients are significantly lower than those of non-internal medicine patients. The elderly and diabetes workers are more likely to develop serious COVID-19 [11].

In summary, PF and TM have demonstrated their advantages in various fields, with sufficient advantages in feature extraction and object recognition. But for SR, a stable and accurate self-localization is needed to identify objects within the field at the determined boundary of the site. Therefore, this study proposes a LD model based on MCPF and TM SR for global region self-localization, in order to achieve global LD in various application scenarios. The innovation of this research is that Monte Carlo particle filter and template matching algorithm are combined in a unique way to improve the positioning detection ability of soccer robots. This model not only broadens the range of Monte Carlo particle filter application scenarios in intelligent robots, but also optimizes the adaptability of template matching to cope with complex moving environments. This study provides new theoretical support and empirical data for understanding and further improving the research on robot positioning. At the same time, it is expected to have a positive impact on the field of machine vision and artificial intelligence, and further promote scientific and technological progress in these fields.

The flowchart of the fusion of the two methods in the paper is shown in Figure 1.

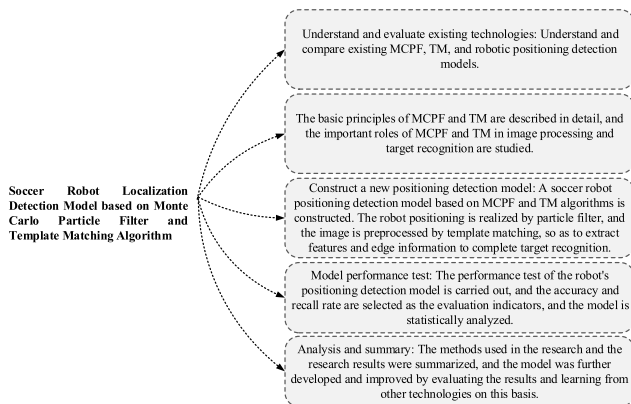


FIGURE 1. Fusion flowchart of MCPF and template matching methods.

III. CONSTRUCTION OF LD MODEL BASED ON MCPF AND TM

The focus of robot LD is on robot machine vision, which is global positioning and navigation based on vision. In SR competition, based on the competition's requirements for real-time and accuracy, this study focuses on image processing and self-localization [12]. Robot positioning is to determine the robot position relative to the given map environment, which is a model of the environment where the machine is located. However, this relies heavily on wireless signals, and when wireless signals cannot be reached, robot's positioning will lose its working ability, resulting in limited application scenarios [13]. Therefore, this study utilizes PF and TM for feature extraction and self-localization processing of target information to improve the efficiency of LD.

A. MCPF LOCALIZATION ALGORITHM

Whether it is a wheeled robot or a humanoid robot, self-localization is generally achieved through PF, which is a basic statistical tool that focuses on probability statistics of position samples and achieves localization through iteration. PF can not only solve the problem of robots changing positions, but also effectively solve nonlinear and non-Gaussian problems [14]. Monte Carlo positioning algorithm is a kind of PF developed on the basis of Bayes, which is mainly composed of prediction and correction, and can realize the global positioning of robots in standard platform group competitions. Figure 2 shows the specific steps of Monte Carlo positioning.

Monte Carlo method is a very flexible and effective numerical calculation method based on probability, which can be used to solve calculation problems randomly. It is mainly through a large number of random samples to analyze the system framework to obtain the desired calculation value. It can be divided into three steps, namely, constructing the probability process, sampling from the known probability distribution, and establishing estimator [15]. MCPF local-

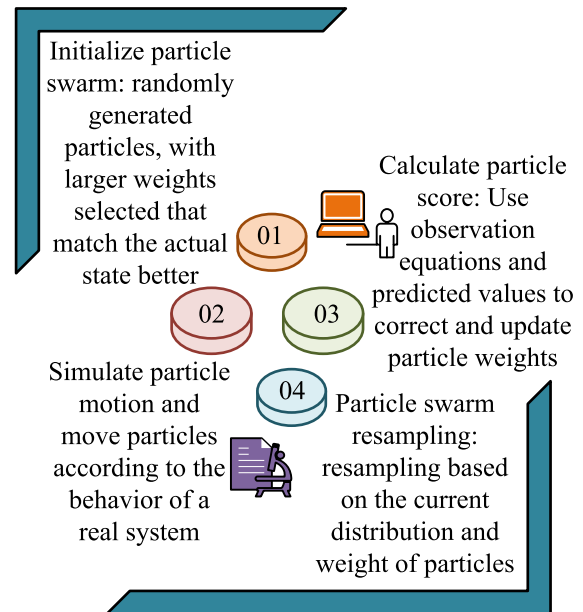


FIGURE 2. Monte carlo localization.

ization is a recursive estimation problem in the state of nonlinear, non-Gaussian dynamic systems, using a limited set of weighted particles to represent posterior probability density of any state. The observation value at t time is updated, and the Prior probability density in the previous step is modified to realize the transfer of prior probability $P(x_t | y_{1:t-1})$ to posterior probability $P(x_t | y_{1:t})$. However, the observation y_t of each system is independent through Markov in Formula (1).

$$P(y_t | y_{1:t-1}, x_t) = P(y_t | x_t) \quad (1)$$

Equation (2) is the transfer update of prior probability density at $t - 1$ time to posterior probability density at t time.

$$P(x_t | y_{1:t}) = \frac{P(y_t | x_t)P(x_t | y_{1:t-1})}{P(y_t | y_{1:t-1})} \quad (2)$$

This method corrects the predicted value through the current observation data to obtain the current state. When robot position changes in real time, posterior probability is constantly updated to be closer to the actual information. Figure 3 shows the specific implementation process of PF algorithm.

There are five steps in MCPF localization. The first step is to initialize all particles with the same weight. The weight is larger, it more matches the actual state. And this study sets the robot's position coordinate as (x, y) and state variable as θ . The second step is to move the particles according to the real system behavior to realize the next state prediction. By using N weighted sampling particle set $S = \{s_i, m_i | i = 1, \dots, N\}$ to represent posterior probability distribution of robot position, Formula (3) is the calculation expression.

$$P(x_k | z_{1:k}) = \frac{P(z_k | x_k)P(x_k | z_{1:k-1})}{P(z_k | z_{1:k-1})} \quad (3)$$

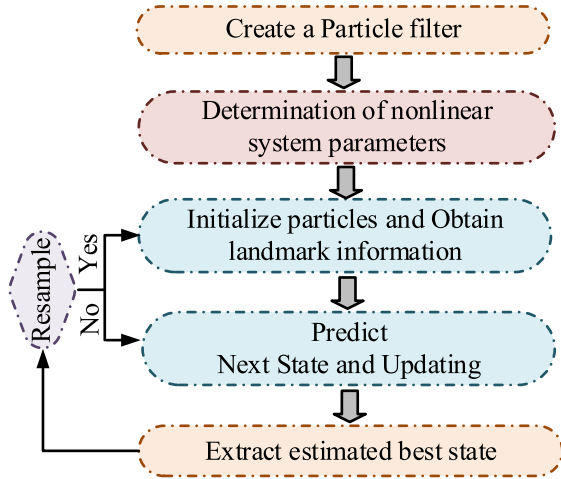


FIGURE 3. Particle filter algorithm.

In equation (3), x_k represents the observed value, z_k represents the state quantity. For each particle, its distribution $P(x_k | z_{1:k})$ can be obtained through the observation equation. The third step is to use observation equations and predicted values for correction, and update the weight of particles based on the measured values to ensure that particles closer to their true positions receive greater weight. Assuming that the probability of obtaining the observation data z at x position at the current time is $P(z | x)$, then Posterior probability is $P(x | z)$. The particle weights were updated through observation data in equation (4).

$$w_k^i = w_{k-1}^i \frac{P(z_k | x_k^i)P(x_k^i | x_{k-1}^i)}{q(x_k^i | x_{k-1}^i, z_{1:n})} \quad (4)$$

In equation (4), $q(x_k^i | x_{k-1}^i, z_{1:n})$ represents the importance density function. The fourth step is to trigger resampling based on the current particles distribution and their weights to retain particles with high weights. To improve computing power and ensure real-time performance, M resamples were performed according to weight size, resulting in the predicted distribution in equation (5).

$$\hat{P}(x_k | z_{1:k-1}) = \sum_{i=1}^M P(x_k | s_k^i, u_{k-1}) \quad (5)$$

In formula (5), s_k^i is the sampling data and $P(z_k | s_k^i, u_{k-1})$ is the observation equation. If the effective particle number is smaller, the weight degradation is more serious. When it is less than a certain threshold, resampling is performed. The fifth step is to calculate the estimated value, calculate this group's particles weighted average and covariance to obtain the probability of this robot at the current position. If the time is longer, the degradation of values will be more severe, and invalid particles will increase. At this point, resampling is necessary to retain particles with higher weights and discard particles with lower weights.

B. TM RESEARCH BASED ON FEATURE EXTRACTION AND RECOGNITION

In the standard platform group competition, SR mainly relies on two parts to achieve global positioning: the first is to obtain feature information through the camera, and the second is to record the walking route through the odometer. Among them, odometer is a variable that accumulates over time. Due to the uncontrollable variable of time, there may be significant errors when recording the distance traveled using a odometer [16]. Therefore, it is necessary to obtain visual information for real-time correction, so visual information is the most important source of information that can be obtained in competitions. The processing of images is an important factor that directly affects the accuracy of robot positioning, and only by doing well in image processing can people more effectively extract site features. Figure 4 shows the specific process of image processing.

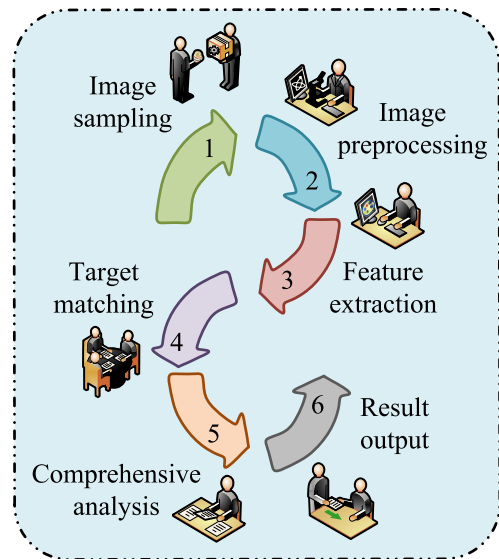


FIGURE 4. Image processing process.

After effectively processing the image, it is necessary to perform target recognition on feature information. However, there are rich and complex features in the environment. If feature's edge information is obvious, it is suitable to extract their straight line features. However, for the visual function of robots, template matching is often required to find objects, and feature point matching is not suitable for robot visual search. Therefore, this study adopts edge based TM [17], [18]. There are two main types of existing TMs. First, they are based on grayscale matching, with the core being to translate template edges in the target image to achieve the calculation of gradient intensity correlation corresponding to edge points [19]. Figure 5 shows the grayscale image template matching process.

This algorithm has strong resistance to white noise. But when the computational object is mixed with other objects, it increases the algorithm computational complexity, resulting in computational errors and affecting real-time per-



FIGURE 5. Image display based on gray value image processing.

formance. Next is feature based template matching, which essentially utilizes geometric features for matching. Due to the freedom to choose geometric features, this method has multiple application scenarios and better real-time performance. This method obtains the sum of normalized dot products of gradient vectors in the image during matching, and then searches for the image. Equation (6) calculates the score of each point in search image.

$$S_{u,v} = \frac{1}{n} \sum_{i=1}^n \frac{(G_{x_i}^T \cdot G_{x(u+X_i, v+Y_i)}^S) + (G_{y_i}^T \cdot G_{y(u+X_i, v+Y_i)}^S)}{\sqrt{G_{x_i}^{T^2} + G_{y_i}^{T^2}} \cdot \sqrt{G_{x(u+X_i, v+Y_i)}^{S^2} + G_{y(u+X_i, v+Y_i)}^{S^2}}} \quad (6)$$

In equation (6), $G_i^T = (G_{x_i}^T, G_{y_i}^T)$ represents the gradient in X and Y directions. i is taken from 1 to n . nEE is the elements number in template (T) dataset. The gradient of search (S) was $G_{u,v}^S = (G_{x(u,v)}^S, G_{y(u,v)}^S)$. The value range of u is rows number in search image. The range of v values is columns number in search image. If it is necessary to accelerate the search speed, it needs to find similar regions and set a minimum (S^{\min}) for similarity measure. To detect the partial score at the specific point J , it is necessary to find the partial sum in equation (7).

$$Sm_{(u,v)} = \frac{1}{m} \sum_{i=1}^m \frac{(G_{x_i}^T \cdot G_{x(u+X_i, v+Y_i)}^S) + (G_{y_i}^T \cdot G_{y(u+X_i, v+Y_i)}^S)}{\sqrt{G_{x_i}^{T^2} + G_{y_i}^{T^2}} \cdot \sqrt{G_{x(u+X_i, v+Y_i)}^{S^2} + G_{y(u+X_i, v+Y_i)}^{S^2}}}$$

$$\times (m \leq n) \quad (7)$$

In equation (7), when $S_m > S^{\min} - 1 + m/n$, the remaining term of sum is less than or equal to 1, the calculation stops. When $S_m > S^{\min} \cdot m/n$, the sum of any point is greater than the minimum value, and this condition is met, the matching speed will be very fast. But if the missing part of object is detected first, there will be a mismatch between detection and template. Therefore, this study combines these two methods to achieve fast and accurate matching in equation (8).

$$Sm < MIN((S^{\min} - 1 + \frac{1-g \cdot S^{\min}}{1-g} \cdot \frac{m}{n}), (S^{\min} \cdot \frac{m}{n})) \quad (8)$$

In equation (8), g is the greedy parameter. If $g = 1$, the template matching points are detected by using equation (7). When $g = 0$, the template matching points are detected using equation (6). As a result, the algorithm normalizes the gradient vector, and this template has illumination invariance. Even when mixed with other objects, it still has high robustness. To accelerate search speed, template matching was optimized using an image pyramid in Figure 6.

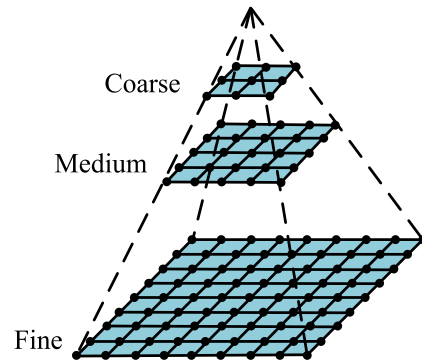


FIGURE 6. Image pyramid structure.

Image pyramid is an effective structure for interpreting images with multiple resolutions, which is a set of images arranged in a pyramid shape with gradually decreasing resolution [20], [21]. The essence of this method is to reduce the resolution of template and search image for easy matching, with the smaller image size located at the top of pyramid. This study continues to search down in this way until it reached the original image size, which is the bottom of pyramid. If the search at the top pyramid is unsuccessful, the next search will be stopped. The use of pyramid models not only accelerates matching speed, but also enhances results accuracy to a certain extent.

C. A ROBOT LD MODEL BASED ON MCPF AND TM

To achieve robot self-localization in standard platform group competitions, a combination of visual perception and algorithms is required. However, due to the symmetry of the field, there may be mirror problems within robot's view field, resulting in robot being unable to distinguish between the enemy and ours [22], [23]. Therefore, based on the implementation of MCPF and TM, real-time communication and

positioning information transmission with teammates can improve the mirroring problem caused by site symmetry. Introducing a team ball model to achieve visual sharing, even if all robots cannot see the ball, they can only find the position information of ball through the forward position. Firstly, it is necessary to construct a global ball model so that this robot can search for the ball through its own view field and its teammates' view field. Figure 7 shows the global sphere model.

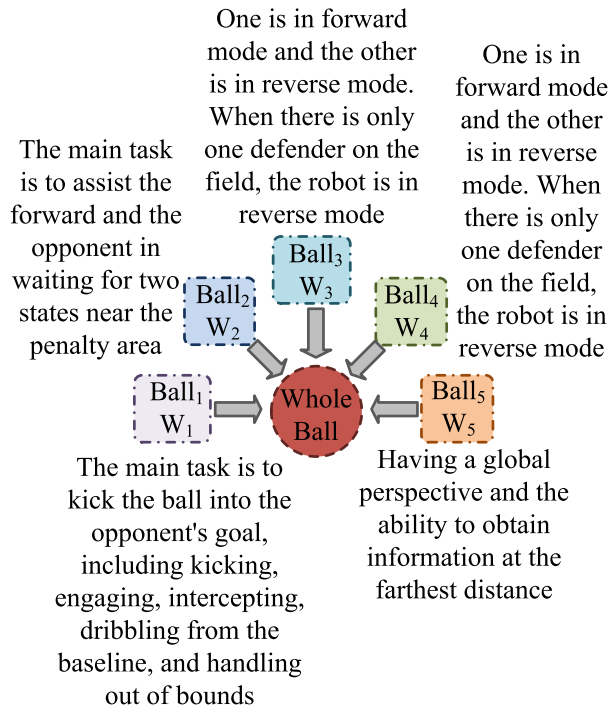


FIGURE 7. Establishment of global sphere model.

There are three factors considered for weight in the global ball model, namely the distance from this ball, ball position in the image, and model's weight seen by different characters. An effective ball model is that each robot has its own ball model $Ball_i(x_i, y_i)$, where i is built based on player's character. If there is no sphere in view field, this sphere model becomes invalid, $Ball_i(x_i, y_i) = (0, 0)$. And there is only one global sphere model $WholeBall(wx_i, wy_i)$. Therefore, the global sphere model is obtained through weighted averaging. The effective independent sphere models number is n . And the global sphere model $WholeBall(wx_i, wy_i)$ is obtained from the independent sphere model $Ball_i(x_i, y_i)$ and weight W . Equation (9) is the calculation.

$$WholeBall = \frac{1}{n} \sum_{i=1}^n w_i Ball_i \quad (9)$$

Based on the combination of MCPF and TM, all visual underlying information required for communication has been constructed. Robots achieve information sharing among robots through the exchange of observation information. By converting between absolute and relative coordinates, the

global area view coverage of the ball model is achieved, and self-positioning information is shared and used with teammates. To ensure the reception of team member information, messages are transmitted through communication, which mainly includes TCP and UDP. UDP is applied in various scenarios with the advantages of simplicity and fast transmission speed, ensuring real-time communication of robots. Figure 8 shows its communication mechanism.

The foundation of team communication is to embed message queues into UDP, and transmit all messages to GameController using UDP based on the robot number, and then transmit them to each robot using GC. The robot itself may have some deviation between ball model and global ball model, so calibration is used to convert global ball model coordinates into robot's coordinates to form an observation equation. The global coordinate of field for this global sphere model is $Ball = [ball_x, ball_y]^T$, and the observation information of robot is $z = [ball_r, ball_\phi]^T$. Equation (10) is the observation equation established for this global sphere model.

$$\begin{bmatrix} ball_r \\ ball_\phi \end{bmatrix} = \begin{bmatrix} \sqrt{(ball_x - x)^2 + (ball_y - y)^2} \\ \arctan(\frac{ball_y - y}{ball_x - x}) \end{bmatrix} \quad (10)$$

SR uses visual information to identify and self-locate the boundary of the field, penalty area, central park, and penalty light road signs. For global positioning of road signs, the distance r and angle ϕ between road signs and robot can be obtained. The coordinates of the road signs are set as $y = [p_x, p_y]^T$, and the observation data is $z = [r, \phi]^T$. Equation (11) represents the observation equation.

$$\begin{bmatrix} r \\ \phi \end{bmatrix} = \begin{bmatrix} \sqrt{(p_x - x)^2 + (p_y - y)^2} \\ \arctan(\frac{p_y - y}{p_x - x}) \end{bmatrix} \quad (11)$$

In equation (11), (x, y) represents the position obtained by robot through motion equations. And noise $w = (w_r, w_\phi) \sim N(0, V)$ satisfying normal distribution also exists in the observed values. Equation (12) represents the observation equation containing noise.

$$\begin{bmatrix} r \\ \phi \end{bmatrix} = \begin{bmatrix} \sqrt{(p_x - x)^2 + (p_y - y)^2} \\ \arctan(\frac{p_y - y}{p_x - x}) \end{bmatrix} + w \quad (12)$$

Equation (13) is expressed in functional form.

$$z_{k,j} = h(y_j, x_k, w_{k,j}) \quad (13)$$

In equation (13), y is the observation value, x is the positioning information, and w is the noise. The overall positioning model of robot is obtained from the observation model in equation (14).

$$\begin{cases} x_k = f(x_{k-1}, \delta_{k-1}, v_{k-1}) \\ z_{k,j} = h(y_j, x_k, w_{k,j}) \end{cases} \quad (14)$$

The positioning model is a nonlinear model, and MCPF can effectively solve the nonlinear problem, thereby obtaining the robot positioning information on the court. However, when

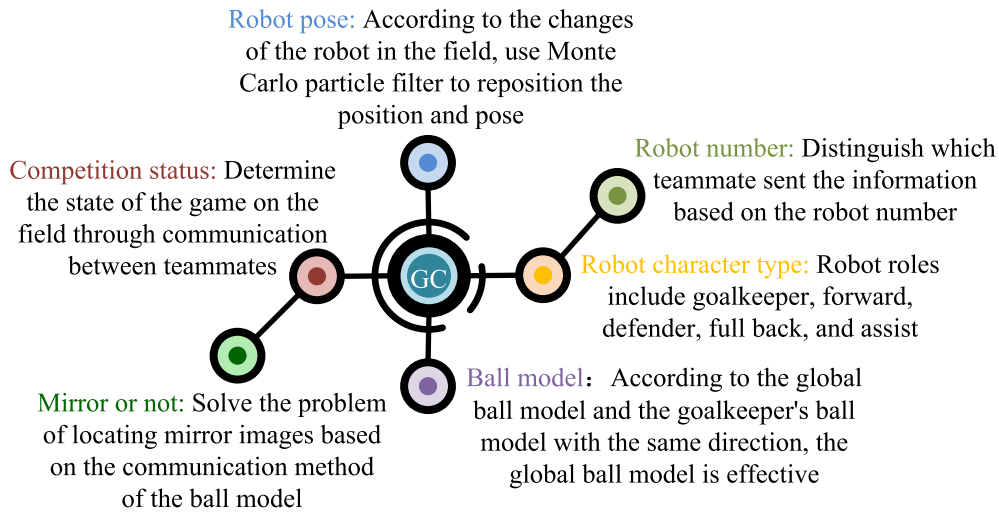


FIGURE 8. IRobot communication mechanism structure.

TABLE 1. Image dataset.

Image Dataset	
Data set	Type
Dataset 1	Original
Dataset 2	Add 10000 random Salt-and-pepper noise
Dataset 3	Add Gaussian blur with Gaussian kernel size of 5
Dataset 4	Rotate the image within the range of -50° with a rotation step size of 1

the positioning result of the first landmark does not appear in the image, this robot observes based on the model to obtain the updated position. The use of a global ball model for global positioning has good correction effects. Due to the weight factor in observation results obtained under ball model, it effectively solves the problem of robot mirroring in games and improves ball model's accuracy.

IV. PERFORMANCE ANALYSIS OF LD MODEL BASED ON MCPF AND TM

To verify the feasibility and effectiveness of LD model based on MCPF and TM, simulation experiments were conducted on this model and the traditional LD model. The experimental environment for this experiment is as follows: a network system is used to search for data, which is used as the experimental parameter for this experiment. The system data are processed using filtering methods. The input serial port is connected through a serial port, with $N-2$ cycles of data. The network interface is data interface, which uses data reading for communication instructions. Operating system is Windows 10, with Intel Core i5-6300 (2.30GHz) CPU and 8GB of memory. In addition, for TM accuracy and matching speed test, four data sets will be used, as well as Gaussian blur, Salt-and-pepper noise, lighting, rotation and other interferences in Table 1.

Table 1 shows the image dataset for TM testing. It mainly consists of four datasets, among which dataset 1 is the original image, which is used as a reference dataset for comparison. The remaining data sets are experimental data. Ten thousand random salt-and-pepper noise are added to data set 2. A Gaussian model with a Gaussian kernel size of 5 is added to data set 3. An image is rotated in an environment with a rotation step of 1° and a range of -50° to data set 4. Figure 9 shows the experimental results under Gaussian blur of this dataset.

According to Figure 9, the mean values generated by these three methods with template size under Gaussian blur are all normal distribution. In Figure 9 (a), Gaussian blur degree of feature edge information under low gradient increases with the template size, and the average value reaches the peak when template size is about 30. Among them, the peak value of MCPF algorithm is the highest at 0.91, followed by TM algorithm at 0.52, while the peak value of MCPF-TM algorithm is the lowest at 0.37. However, Gaussian blur of feature edge information under strong gradient is lower than that under low gradient image processing. The peak value of MCPF algorithm is the highest at 0.70, followed by TM algorithm at 0.31, while the peak value of MCPF-TM algorithm is the lowest at 0.14. Therefore, the degree of Gaussian blur is lower under the feature edge information of low gradient, and the result of image processing is clearer. When salt-and-pepper noise is selected to process the image, Figure 10 shows the result.

Figure 10 shows the changes of the overall SNR in the original image and the image processing after adding salt and pepper noise. When no noise is added, in FIG. 10 (a), the SNR of MCPF algorithm when processing the original image is the lowest compared with other algorithms. In general, it can be seen that the SNR value of the initial edge is 0.062. The SNR after TM algorithm is reduced by 0.04 compared with the initial value. In contrast, the variation of SNR after MCPF-TM algorithm is relatively small, and the SNR results

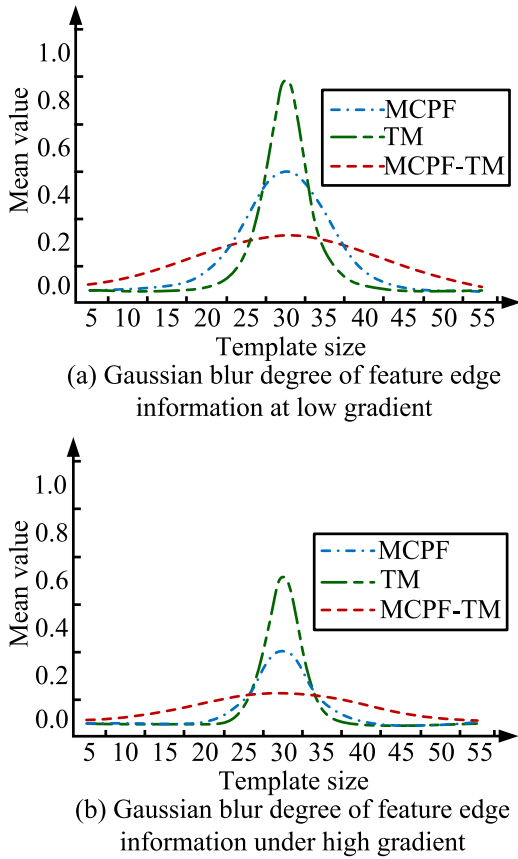


FIGURE 9. IRobot communication mechanism structure.

of each edge are relatively close. In FIG. 10 (b), when pepper and salt noise is added to the image, all the SNR values after processing are higher than those when processing the original image. The MCPF algorithm shows a significant increase in SNR, and the SNR value at the initial edge is 0.11. The SNR value of TM algorithm shows a trend of first increase and then decrease, but the overall change is not obvious. However, the MCPF-TM algorithm shows an upward trend, from the initial SNR value of 0.27 to 0.35, with an increase of 0.08 at the edge. It can be seen that after adding salt and pepper noise, the SNR value of image processing increases, but the recognition rate of image decreases.

According to Figure 11, the accuracy of image recognition was tested under both strong and weak light conditions, and the overall results showed an upward trend. Under weak lighting conditions in Figure 11 (a), each algorithm increases with test number. The accuracy of image recognition under MCPF algorithm increased from 0.02 to 0.73, and the accuracy of image recognition under TM algorithm increased from 0.06 to 0.82. The accuracy of image recognition under MCPF-TM algorithm is 0.07, and the initial accuracy is higher than that of the first two algorithms. As test number increases, the accuracy of image recognition increases to 0.91. Under strong lighting conditions in Figure 11 (b), as test number increases, each algorithm has

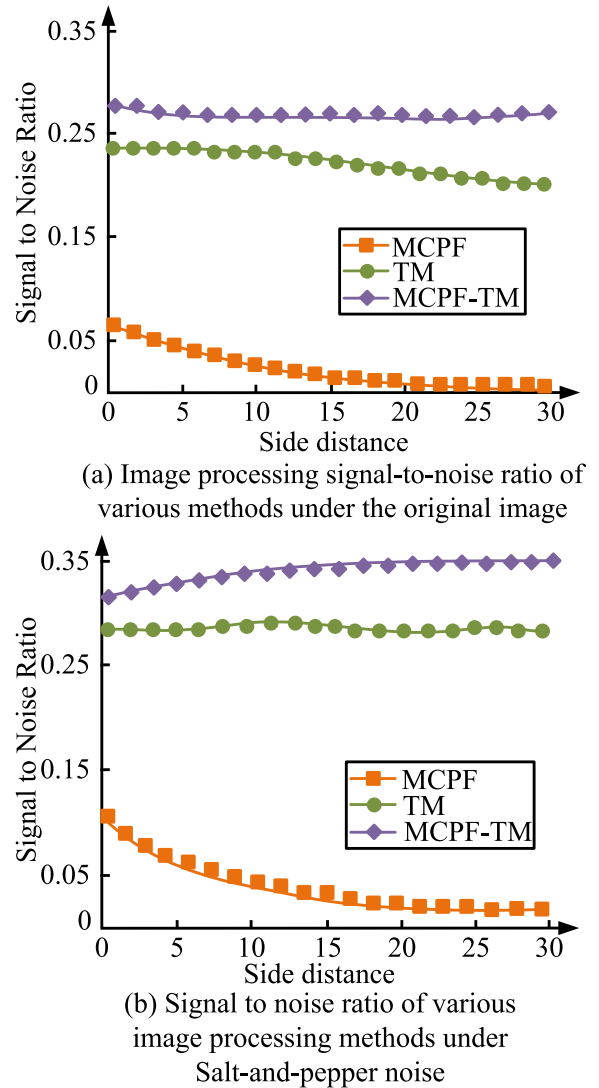


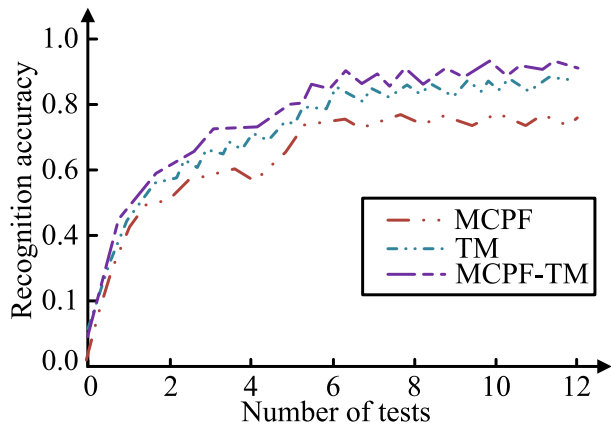
FIGURE 10. SNR curve of image processing under Salt-and-pepper noise.

a higher accuracy in image recognition compared to weak lighting conditions. The accuracy of image recognition under MCPF algorithm increased from 0.01 to 0.84, and the accuracy of image recognition under TM algorithm increased from 0.04 to 0.92. The accuracy of image recognition under MCPF-TM algorithm is 0.08, and the initial accuracy is higher than that of the first two algorithms. As test number increases, its recognition accuracy for images increases to 0.97. Therefore, MCPF-TM algorithm has a higher accuracy in image recognition under strong lighting conditions than under weak lighting conditions. Table 2 shows the image processing results of several algorithms in different experimental environments.

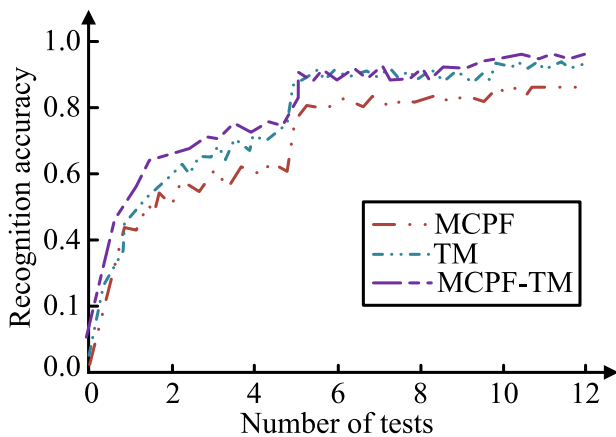
According to Table 2, the accuracy of image processing under local noise interference is related to template size. The template size are closer the length and width, image contains more pixels, and the accuracy of image processing is higher. Based on MCPF and template algorithms, a lot of processing

TABLE 2. Algorithm comparison.

Algorithm	Template drawing size	Original image	Care changes	Gaussian	Salt-and-pepper noise	Rotate	Average time consumption
MCPF	200*200	93.36	81.23	90.88	92.39	58.33	99.16
	210*125	94.02	86.32	91.41	93.61	67.34	99.32
TM	200*200	86.16	91.61	88.78	93.59	78.46	99.06
	210*125	88.24	95.36	89.59	96.57	84.31	99.25
MCPF-TM	200*200	98.12	98.667	99.34	98.59	94.81	99.13
	210*125	99.56	99.16	99.47	99.02	95.75	99.67



(a) Image recognition curves of various methods under low light conditions

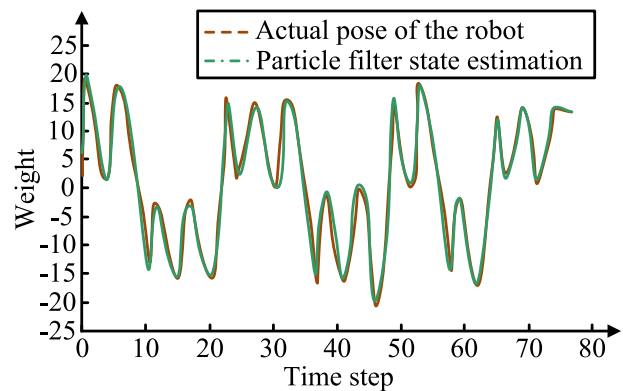


(b) Image recognition curves of various methods under strong light conditions

FIGURE 11. Accuracy curve of image recognition under strong and weak lighting conditions.

has been carried out on the search graph, especially in the rotated image, where the top-level step size is set smaller to avoid slow matching speed caused by incorrect matching and increase the matching accuracy of this algorithm. Moreover, the performance of estimation method is relatively stable under various interferences, and its template matching speed is good. MCPF-TM algorithm also has high accuracy in image processing results and high robustness to changes in lighting. This study used MCPF algorithm to perform LD on robots, and in this experiment, approximately 1000 frames of

images were taken. Figure 12 shows the simulation experiment results.

**FIGURE 12.** Robot positioning detection result curve based on Monte Carlo particle filter algorithm.

In Figure 12, algorithm weight exhibit waveform changes over time. At the beginning of test, the weight value of robot's actual pose is 2. Whentime step is 80, the weight value of robot's actual pose is 14. Throughout the testing process, the highest weight value of robot's overall posture was 19, and the lowest weight value was -21 . The weight values of PF state estimation are as high as 20 and as low as -19 throughout the entire process. Among them, under good recognition conditions, the positioning accuracy of MCPF algorithm is greater than 94%. When recognition environment is poor or there is a lot of external noise, the accuracy of MCPF algorithm is about 72%. As a result, particles are always near the robot position, and state estimation is also relatively close to the actual pose of this robot, with a small deviation. You Only Look Once (YOLO), Sequential Similarity Detection Algorithms (SSDA), Normalized Cross Correlation (NCC), and MCPF-TM algorithm proposed in this study were selected to test the accuracy of machine human LD model in Figure 13.

According to Figure 13, the estimation results of robot LD under all four algorithms show an upward trend. In Figure 13 (a), YOLO algorithm has the lowest LD result for robots with an accuracy of 0.864, while MCPF-TM algorithm has the highest LD result with an accuracy of 0.882. Among them, YOLO algorithm tends to be stable when tested 389 times, SSDA algorithm tends to be stable when tested 412 times, NCC algorithm tends to be stable when tested 378 times, and MCPF-TM algorithm tends to be stable

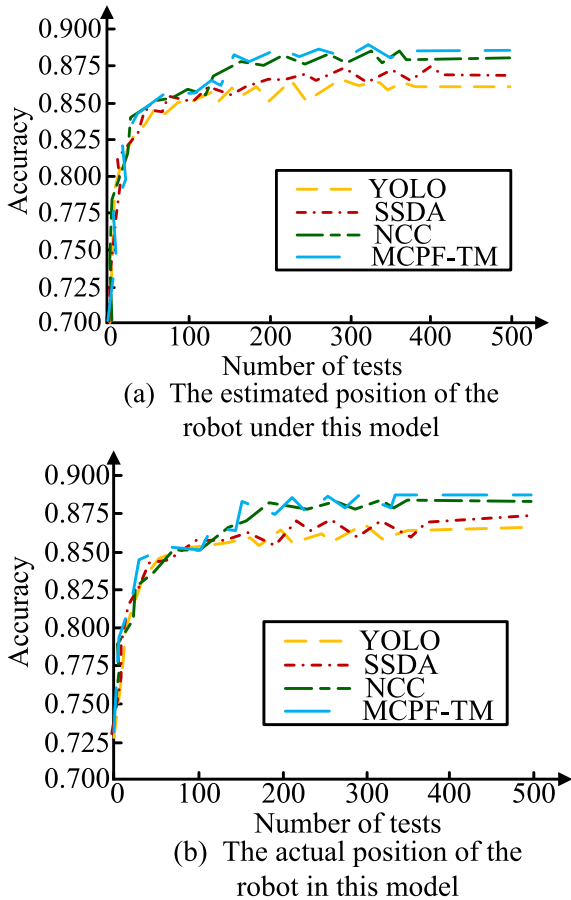


FIGURE 13. Accuracy curve of location detection model based on Monte Carlo particle filter and template matching algorithm.

when tested 376 times. In Figure 13 (b), the actual LD results of the robot under the four algorithms are initially higher than the estimated position results. YOLO algorithm still has the lowest LD result for robots with an accuracy of 0.872, while MCPF-TM algorithm has the highest LD result with an accuracy of 0.895. The recall rates of these four algorithms were tested in Figure 14.

According to Figure 14, the actual value's recall rate is roughly the same compared to the estimated value. In Figure 14 (a), robot LD model's recall rate under YOLO algorithm is the lowest. As recall rate increases to 0.96, its accuracy decreases to 0.32 and the accuracy is 0.95. MCPF-TM algorithm has the highest recall rate, with an accuracy of 0.97. When the recall rate increases to 0.96, its accuracy is 0.33. In Figure 14 (b), robot LD model's recall rate under YOLO algorithm is the lowest, and as the recall rate increases to 1, the accuracy decreases to 0.41. MCPF-TM algorithm has the highest recall rate, with an accuracy of 0.99. When the recall rate increases to 1, the accuracy of this algorithm is 0.43. Therefore, MCPF-TM algorithm has the highest accuracy in recall rate. Whether in the estimated or actual values, and the recall accuracy index of the estimated and actual values is roughly the same, verifying

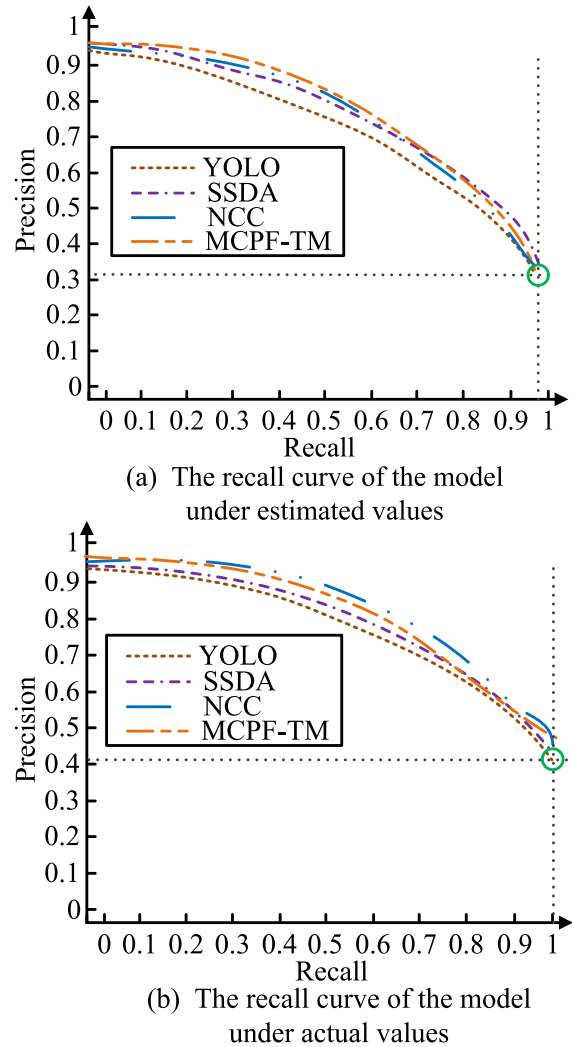


FIGURE 14. Recall rate curve of location detection model based on Monte Carlo particle filter and template matching algorithm.

the effectiveness and feasibility of LD model under this algorithm.

V. CONCLUSION

Artificial intelligence technology builds intelligent systems for people to solve problems on their own, such as humanoid robots. Intelligent robots are designed to imitate human form and behavior, understand and adapt to the environment, and perform precise and flexible operations. The artificial intelligence technology is used to realize the global positioning of the robot in the humanoid SR competition, and the technology of image processing, pattern recognition and multi-machine communication is integrated. Based on this, the performance test of LD model based on Monte Carlo particle filter and template matching algorithm is proposed and carried out to solve the global positioning problem of SR. In the process of large-scale processing search images, especially in the process of rotating images, a small top-level step is set to avoid the matching speed due to matching errors and improve

the matching accuracy. In addition, the performance of the verification method is relatively stable under various disturbances, and the template matching speed is good. MCPF-TM algorithm has good accuracy in image processing results and robustness to illumination changes. In the test process, the highest and lowest weight values of the robot's overall attitude are 19 and -21 , respectively, and the highest and lowest weight values of the PF state estimation are 20 and -19 , respectively. Under good recognition conditions, the positioning accuracy of MCPF algorithm is greater than 94%, and in noisy environment, the accuracy is about 72%. Therefore, the particle is always near the position of the robot, and the state estimate is relatively close to the actual posture of the robot, with small deviation. However, SR robots are only one class of robots, there are wheeled robots, service robots, and other types of mobile robots in real life. Therefore, it is necessary to further study and explore the applicability of the algorithm proposed in this work on other types of robots.

REFERENCES

- [1] L.-E. Montoya-Cavero, R. D. de León Torres, A. Gómez-Espinosa, and J. A. E. Cabello, "Vision systems for harvesting robots: Produce detection and localization," *Comput. Electron. Agricult.*, vol. 192, Jan. 2022, Art. no. 106562.
- [2] Z. Zhou, L. Li, A. Fürsterling, H. J. Durocher, J. Mouridsen, and X. Zhang, "Learning-based object detection and localization for a mobile robot manipulator in SME production," *Robot. Comput.-Integr. Manuf.*, vol. 73, Feb. 2022, Art. no. 102229.
- [3] F. Wu, J. Duan, P. Ai, Z. Chen, Z. Yang, and X. Zou, "Rachis detection and three-dimensional localization of cut off point for vision-based banana robot," *Comput. Electron. Agricult.*, vol. 198, no. 2, Jul. 2022, Art. no. 107079.
- [4] W. Guo, W. Hu, C. Liu, and T. Lu, "Pose initialization of uncooperative spacecraft by template matching with sparse point cloud," *J. Guid., Control, Dyn.*, vol. 44, no. 9, pp. 1707–1720, Sep. 2021, doi: 10.2514/1.G005042.
- [5] C. Wu and Z. Li, "Local thinning of 3D stereo images based on symmetric decryption algorithm," *Microprocess. Microsyst.*, vol. 82, Apr. 2021, Art. no. 103803, doi: 10.1016/j.micpro.2020.103803.
- [6] Z. Jiao, Z. Feng, N. Lv, W. Liu, and H. Qin, "Improved particle filter using clustering similarity of the state trajectory with application to nonlinear estimation: Theory, modeling, and applications," *J. Sensors*, vol. 2021, May 2021, Art. no. 9916339, doi: 10.1155/2021/9916339.
- [7] Q. Liu, X. Di, and B. Xu, "Autonomous vehicle self-localization in urban environments based on 3D curvature feature points—Monte Carlo localization," *Robotica*, vol. 40, no. 3, pp. 817–833, Mar. 2022, doi: 10.1017/S0263574721000862.
- [8] J. J. Steckenrider and T. Furukawa, "Simultaneous estimation and modeling of nonlinear, non-Gaussian state-space systems," *Inf. Sci.*, vol. 578, pp. 621–643, Nov. 2021, doi: 10.1016/j.ins.2021.06.097.
- [9] M. Ballesio and A. Jasra, "Unbiased estimation of the gradient of the log-likelihood for a class of continuous-time state-space models," *Monte Carlo Methods Appl.*, vol. 28, no. 1, pp. 61–83, Feb. 2022, doi: 10.1515/mcma-2022-2105.
- [10] B. Hu, Q. Yu, and H. Yu, "Global vision localization of indoor service robot based on improved iterative extended Kalman particle filter algorithm," *J. Sensors*, vol. 2021, Jul. 2021, Art. no. 8819917, doi: 10.1155/2021/8819917.
- [11] Y. Zheng, Q. Zeng, C. Lv, H. Yu, and B. Ou, "Mobile robot integrated navigation algorithm based on template matching VO/IMU/UWB," *IEEE Sensors J.*, vol. 21, no. 24, pp. 27957–27966, Dec. 2021, doi: 10.1109/JSEN.2021.3122947.
- [12] S. Liang and Y. Li, "Using Camshift and Kalman algorithm to trajectory characteristic matching of basketball players," *Complexity*, vol. 2021, Jun. 2021, Art. no. 4728814, doi: 10.1155/2021/4728814.
- [13] J. Gai, L. Xiang, and L. Tang, "Using a depth camera for crop row detection and mapping for under-canopy navigation of agricultural robotic vehicle," *Comput. Electron. Agricult.*, vol. 188, Sep. 2021, Art. no. 106301.
- [14] X. Zhang, Y. Liu, and X. Wang, "A sparsity preestimated adaptive matching pursuit algorithm," *J. Electr. Comput. Eng.*, vol. 2021, Apr. 2021, Art. no. 5598180, doi: 10.1155/2021/5598180.
- [15] Z. R. Wani, M. Tantray, and E. Norooznejad Farsangi, "In-plane measurements using a novel streamed digital image correlation for shake table test of steel structures controlled with MR dampers," *Eng. Struct.*, vol. 256, Apr. 2022, Art. no. 113998, doi: 10.1016/j.engstruct.2022.113998.
- [16] Y. Li, W. Wang, K. E. Deng, and J. S. Liu, "Stratification and optimal resampling for sequential Monte Carlo," *Biometrika*, vol. 109, no. 1, pp. 181–194, Feb. 2022, doi: 10.1093/biomet/asab004.
- [17] T. Li and F. Hlawatsch, "A distributed particle-PHD filter using arithmetic-average fusion of Gaussian mixture parameters," *Inf. Fusion*, vol. 73, pp. 111–124, Sep. 2021, doi: 10.1016/j.inffus.2021.02.020.
- [18] Z. Zhou, C. Zeng, X. Tian, Q. Zeng, and R. Yao, "A discrete quaternion particle filter based on deterministic sampling for IMU attitude estimation," *IEEE Sensors J.*, vol. 21, no. 20, pp. 23266–23277, Oct. 2021, doi: 10.1109/JSEN.2021.3109156.
- [19] F. Masood, J. Masood, H. Zahir, K. Driss, N. Mehmood, and H. Farooq, "Novel approach to evaluate classification algorithms and feature selection filter algorithms using medical data," *J. Comput. Cogn. Eng.*, vol. 2, no. 1, pp. 57–67, Jan. 2022, doi: 10.47852/bonviewJCCE2202238.
- [20] P. K. Panigrahi and S. K. Bisoy, "Localization strategies for autonomous mobile robots: A review," *J. King Saud Univ.-Comput. Inf. Sci.*, vol. 34, no. 8, pp. 6019–6039, Sep. 2022.
- [21] A. V. Le, P. T. Kyaw, R. E. Mohan, S. H. M. Swe, A. Rajendran, K. Boopathi, and N. H. K. Nhan, "Autonomous floor and staircase cleaning framework by reconfigurable sTetro robot with perception sensors," *J. Intell. Robot. Syst.*, vol. 101, no. 1, Jan. 2021.
- [22] X. Chen, H. Huang, Y. Liu, J. Li, and M. Liu, "Robot for automatic waste sorting on construction sites," *Autom. Construct.*, vol. 141, Sep. 2022, Art. no. 104387.
- [23] L. Fang and M. Sun, "Motion recognition technology of badminton players in sports video images," *Future Gener. Comput. Syst.*, vol. 124, pp. 381–389, Nov. 2021, doi: 10.1016/j.future.2021.05.036.



LI XIAO was born in Henan, in February 1970. She received the bachelor's degree in physical education from Henan University, in 1992, and the master's degree in master of education in physical education and training, majoring in physical education and training, in 2005.

From 1992 to 2018, she was the Director of the Department of Preschool Education and Arts, Henan Finance and Economics School. Since 2018, she has been a full-time Teacher with the Henan Logistics Vocational College. Her academic works include "Analysis of Innovative Paths for the Reform of Physical Education Teaching in Vocational Schools" (Research), in August 2018, "The Application of Virtual Reality Technology in Physical Education Teaching" (Sports Vision), in April 2021, and "Examining the Reform and Development of School Physical Education in China from the Perspective of Lifelong Physical Education Thought" (Yangtze River Series), in July 2020.

• • •